



LAWRENCE
LIVERMORE
NATIONAL
LABORATORY

Observation of hohlraum-wall motion with spectrally separated X-ray imaging at the National Ignition Facility

N. IZUMI, N. Meezan, L. Divol, G. N. Hall, M. A. Barrios, O. Jones, O. L. Landen, J. J. Kroll, S. Vonhof, A. Nikroo, J. Jaquez, C. Bailey, M. Hardy, R. Ehrlich, R. Pj. Town, D. K. Bradley, D. E. Hinkel, J. D. Moody

July 7, 2016

the 21st Topical Conference on High-Temperature Plasma Diagnostics

Madison, WI, United States

June 5, 2016 through June 9, 2016

Disclaimer

This document was prepared as an account of work sponsored by an agency of the United States government. Neither the United States government nor Lawrence Livermore National Security, LLC, nor any of their employees makes any warranty, expressed or implied, or assumes any legal liability or responsibility for the accuracy, completeness, or usefulness of any information, apparatus, product, or process disclosed, or represents that its use would not infringe privately owned rights. Reference herein to any specific commercial product, process, or service by trade name, trademark, manufacturer, or otherwise does not necessarily constitute or imply its endorsement, recommendation, or favoring by the United States government or Lawrence Livermore National Security, LLC. The views and opinions of authors expressed herein do not necessarily state or reflect those of the United States government or Lawrence Livermore National Security, LLC, and shall not be used for advertising or product endorsement purposes.

Observation of hohlraum-wall motion with spectrally selective X-ray imaging at the National Ignition Facility^{a)}

N. Izumi^{1, b)}, N. Meezan¹, L. Divol¹, G. N. Hall¹, M. A. Barrios¹, O. Jones¹, O. L. Landen¹, J. J. Kroll¹, S. Vonhof¹, A. Nikroo¹, J. Jaquez², C. Bailey¹, M. Hardy¹, R. Ehrlich¹, R. Pj. Town¹, D. Bradley¹, D. E. Hinkel¹, and J. D. Moody¹

¹ Lawrence Livermore National Laboratory, Livermore, California, 94551, USA

² General Atomics, San Diego, California, 9212, USA

(Presented XXXXX; received XXXXX; accepted XXXXX; published online XXXXX)

(Dates appearing here are provided by the Editorial Office)

The high fuel capsule compression required for indirect drive inertial confinement fusion (ICF) requires careful control of the X-ray drive symmetry throughout the laser pulse. When the outer cone beams strike the hohlraum wall, the plasma ablated off the hohlraum wall expands into the hohlraum and can alter both the outer and inner cone beam propagation and hence the X-ray drive symmetry especially at the final stage of the drive pulse. To quantitatively understand the wall motion, we developed a new experimental technique which visualizes the expansion and stagnation of the hohlraum wall plasma. Details of the experiment and the technique of spectrally selective x-ray imaging are discussed.

I. INTRODUCTION

The purpose of the high Z hohlraum is to provide soft-X-ray radiation drive in a symmetric and predictable fashion. However, the motion of the hohlraum wall can dynamically alter the drive asymmetry. The laser irradiation intensity of the hohlraum wall is highest for the outer cone beams. This causes the portion of the hohlraum wall irradiated by the outer cone beams to ablate and produce bubbles of high Z (typically Au or U plasma) [1]. The capsule surface is ablated by the X-ray drive and expands radially. When the high Z bubble and the low Z ablator plasmas collide, a region of high density forms which can absorb laser light and reduce the inner beam power reaching the hohlraum wall.

To provide efficient and effective control of drive asymmetry, quantitative understanding of the hohlraum wall motion is important. Some hohlraum designs with a CH ablator use relatively high initial hohlraum fill pressure (filled with ⁴He, 0.96 ~ 1.6 mg/cc) to tamp and minimize the hohlraum wall motion. However, these higher gas-fill hohlraums have significant backscatter, hot electrons, and require cross-beam energy transfer (CBET) for symmetry control [2-4]. High density carbon (HDC) [5] provides an interesting alternative to this. Because of its high initial density (3.5 g/cc), the initial thickness of the shell is thinner than plastic ablators so the transit time of the shock through the ablator is significantly reduced. This allows implosion designs with much shorter laser pulses (about a factor of 3 shorter than a CH ablator). Due to this shorter drive, expected wall motion is smaller and it opens up possibilities of hohlraum designs with lower gas fill. Currently we are studying the performance of near vacuum hohlraums (NVH) at 0.03 mg/cc and intermediate fill hohlraums (IFH) at 0.3 ~ 0.6 mg/cc. Compare to the standard fill density (0.96 ~ 1.6 mg/cc), these lower gas-fill hohlraums have lower backscatter, lower hot electrons, and do not require CBET for radiation drive symmetry

control. However, due to reduced tamping of the wall plasma expansion, collision between the wall and the ablator plasma may interfere with the propagation of the inner cone beams (through absorption) during the highest intensity part of the main drive pulse. We developed a new experimental technique which visualizes the wall and capsule ablator motion in the hohlraum.

II. EXPERIMENT

Fig. 1 (a) shows the target and laser configuration used in the experiment. The hohlraum (known as “Viewfactor” [6]) has one laser entrance hole (LEH) on the bottom side and a large opening on the top side. The hohlraum is irradiated by 128 NIF beams (all the 96 beams from the bottom side and only the 32 inner cone beams from the top side).

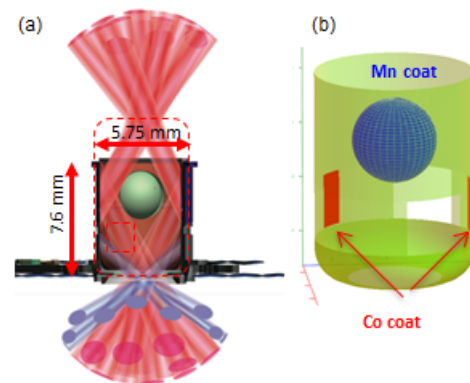


FIG. 1. (a) Model of hohlraum and irradiation pattern. (b) Model of inside. Thin layers of manganese and cobalt are coated on the capsule surface and under the beam spots of Q34B and Q13B, respectively. The hohlraum has two diagnostic holes with HDC windows.

^{a)}Contributed paper published as part of the Proceedings of the 21st Topical Conference on High-Temperature Plasma Diagnostics (HTPD 2016) in Madison, Wisconsin, USA.

^{b)}Author to whom correspondence should be addressed: izumi2@llnl.gov

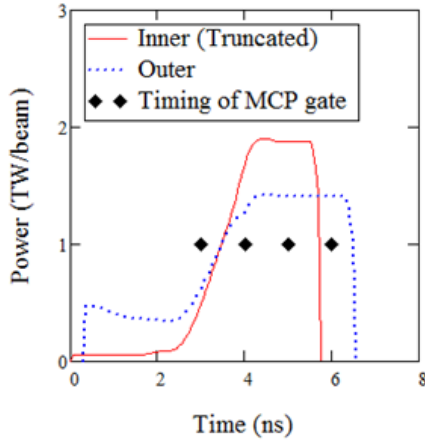


FIG. 2. Laser pulse shape used for the experiment. The diamonds are showing the gate timing of the x-ray imager.

Fig. 1 (b) shows the interior of the target. A cobalt tracer (320 nm thick, shown in red color) is coated on the beam spot under the 50° Q34B and Q13B. To image X-ray line emission from these tracer materials, the hohlraum has two diagnostics windows 2.6 mm below the center of the capsule. To avoid the window closing due to gold plasma expansion, HDC plates (width 2.1 mm, height 2 mm, thickness 166 μm) are installed in the diagnostic windows. The surface of the plastic capsule (outer diameter 2.95mm, thickness 30 μm) was coated with a thin layer of manganese (320 nm thick, shown in blue color). The density of the hohlraum filling gas (neopentane) is set to 0.515 mg/cc to have an electron density equivalent to cryogenic IFHs filled with ^4He at 0.6 mg/cc.

Fig. 2 shows the laser pulse used in this experiment. The inner cone beams are shortened in this case to 5.75 ns in order to reduce the risk of the laser optics damage from possible stimulated backscattering in the high intensity part of the laser pulse. The total energy delivered by the 128 beams is 624 kJ. Images of X-ray emission from the tracer material are obtained with a 100 ps resolution micro-channel plate (MCP) based X-ray framing cameras [7-8]. Fig. 3 shows the diagnostic setup. A pinhole array located 190 mm from the object (hole diameter: 100 μm) casts 16 images onto the MCP (magnification of 2x, resolution = 150 μm).

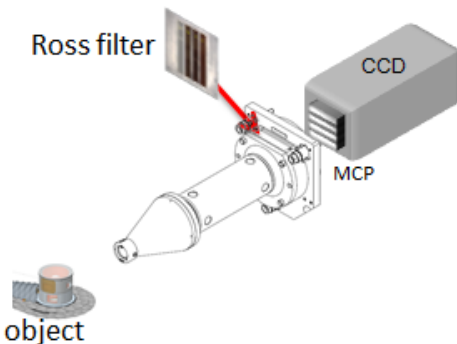


FIG. 3. Set up of the MCP based X-ray framing cameras.

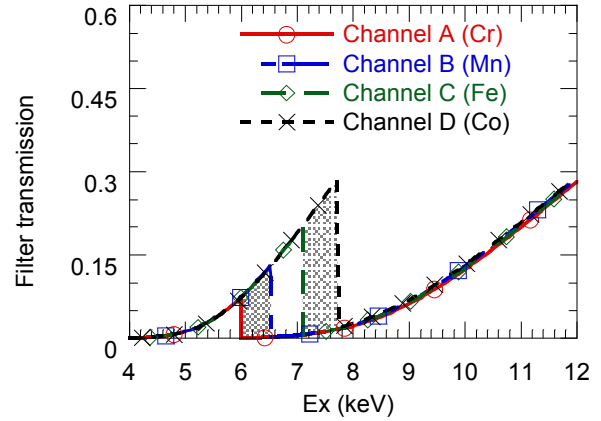


FIG. 4. Transmission of the filter array. Thickness of filter material is adjusted so that transmission of all the channels matches above 7.71 keV. Filter materials used common to all the channels are the HDC window on the hohlraum (166 μm thick) and plastic layers for debris protection (~ 650 μm thick in total).

In order to separate the X-ray emission from the tracer materials, an array of filters consisting of 4 different materials (Cr 17 μm , Mn 15 μm , Fe 25 μm , Co 10 μm) was installed in front of the MCP. Fig. 4 shows the transmission of the filters. The thickness of the 4 filter materials is chosen so that transmission above 7.71 keV is identical for all the channels [9]. By subtracting the channel B images from the channel A, we obtain spectrally selective X-ray images (5.989 ~ 6.54 keV) with signal dominated by He-alpha emission from the Mn (6.2 keV). Subtraction of channel C from D provides image between 7.11~7.71 keV which gives an image dominated by He-alpha emission from the cobalt (7.2 keV). Fig. 5 shows the raw and the subtracted images obtained from the first diagnostic port (polar angle = 90deg, azimuthal angle = 315 deg). This camera sees the expansion of the Co tracer coated under the Q34B spot. The raw images contain both continuum and line x-ray emission. The images of channel A and B are similar except for the region of the ablated capsule (top-left corner of the image). The image after subtraction clearly shows the extent of the Mn tracer. Similarly, subtraction of the channel C from D can visualize the region of the Co tracer. Background due to Au emission is low because opposite side of the hohlraum wall is also the HDC window.

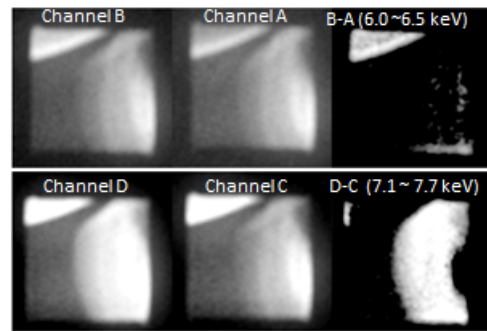


FIG. 5. Images observed from the diagnostic port P90-315 (logarithmic intensity scale, time = 5ns). The images obtained on this line-of-sight contains less background because opposite side of the hohlraum wall is a low-Z window material.

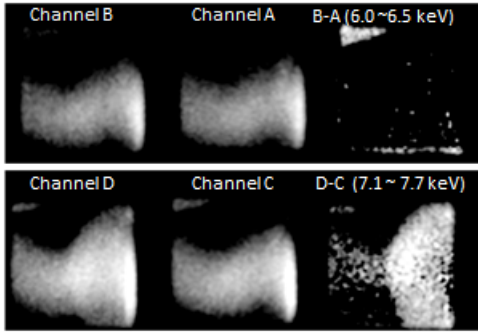


FIG. 6. Images observed from the diagnostic port P90-78 (logarithmic intensity scale, time = 3.5 ns). On channel D, emission from Co tracer is overlapped on background from the laser spots on the gold wall.

Fig. 6 shows the images obtained from the second port (polar angle = 90deg, azimuthal angle = 78.75 deg). This view sees the expansion of the Co tracer under Q13B spot. Because the other side the diagnostic hole is the gold wall, the signal is dominated by emission from the laser spot on the gold wall. Although the resulting images get noisy, it is possible to extract the extent of the tracer plasma by doing the matched pair subtraction.

Fig.7 shows the time evolution of the subtracted images. The blue and the red regions are line emission from the Mn and the Co tracer respectively. The dark region between them is low Z plasma, which originally was neopentane gas (C_5H_{12}) and the plastic window material used on the laser entrance hole.

In the first frame ($t = 3$ ns), the boundary of the Co has a round shape which indicates a radial expansion from the outer cone beam spot. The travel of the Co bubble boundary is 1.3 mm from the hohlraum wall. In the second frame ($t = 4$ ns), the boundary expands to 1.7 mm from the wall. The speed of the bubble expansion between the 1st and 2nd frame is 380 km/sec. On 5ns, the Mn plasma from the capsule surface is start colliding with the Co plasma. The dark region on right hand side is Au plasma which initially was underneath the Co coating. On 6ns, the radial expansion of the Co plasma from the wall is 2.0 mm. The low Z plasma is compressed and the ablator plasma is almost touching the hohlraum bubble.

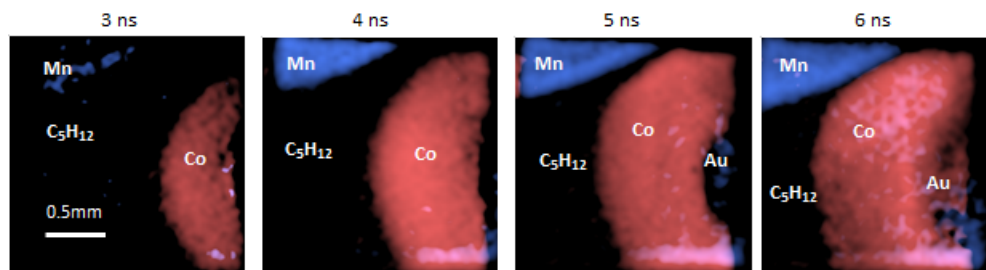


FIG. 7. Time development of the experimentally obtained images (logarithmic intensity scale). X-ray energy between 6.0 ~6.5 keV is shown in the blue and 7.1 ~7.7 keV is shown in red color. Expansion of ablator plasma (Mn) and hohlraum wall bubble (Co) were separated clearly.

III. DISCUSSION

By using the thin layers of the tracer materials and the spectrally selective X-ray imaging, the time development of the material boundaries inside the hohlraum was visualized. The material boundaries were extracted even when the line emission image of the tracer is overlapped onto the emission from the Au wall, although the subtracted images are noisier than that without overlapped Au emission. The laser plasma interaction and hydrodynamic behavior of the wall motion could be altered by the existence of the tracer materials. For example, expansion of the mid-Z tracer can be more than the Au because the tracer has less radiation cooling. In the this experiment, the total expansion of the hohlraum wall under the outer cone spot was 2 mm from the original surface at 6ns and roughly half of its thickness is occupied by the Co plasma. Therefore, the observed expansion of the Co plasma can overestimate the Au wall motion without the Co tracer. This hydrodynamic “surrogacy” issue can be relaxed by reducing the initial thickness of the tracer layer.

IV. ACKNOWLEDGMENTS

This work was performed under the auspices of the U.S. Department of Energy by Lawrence Livermore National Laboratory under Contract DE-AC52-07NA27344.

V. REFERENCES

- ¹M. B. Schneider, S. A. MacLaren, K. Widmann, et al., J. Phys. Conf. Ser. **717** 012049 (2016)
- ²R. P. J. Town, M. D. Rosen, P. A. Michel, et al., Phys. Plasmas **19**, 056302 (2011).
- ³P. Michel, L. Divol, E. Williams, et al., Phys Rev. Lett. **102** 025004 (2009).
- ⁴P. Michel, S. H. Glenzer, L. Divol, et al., Phys. Plasmas **17**, 056305 (2010)
- ⁵A. J. MacKinnon, N. B. Meezan, J. S. Ross, et al, Phys. Plasmas **21**, 056318 (2014).
- ⁶S. A. MacLaren M. B. Schneider, K. Widmann et al., Pys. Rev. Lett. **112** 105003 (2014).
- ⁷J. A. Oertel, R. Aragonéz, T. Archuleta, et al., Rev. Sci. Instrum. **77**, 10E308 (2006).
- ⁸L. R. Benedetti, J. P. Holder, M. Perkins, et al., Rev. Sci. Instrum. **87**, 023511 (2016).
- ⁹P. A. Ross, J. Opt. Soc. Am. **16**, 433 (1928).